Comparing Open Area Test Site and Resonant Chamber for Unmanned Aerial Vehicle's High-Intensity Radiated Field Testing

Sergio Fernández Romero, Patricia López Rodríguez, David Escot Bocanegra, *Member, IEEE*, David Poyatos Martínez, and Manuel Añón Cancela

***Abstract*—Open area test sites (OATS) have been traditionally employed for aircraft electromagnetic compatibility certification tests because of the large size of these items. In this regard, unmanned aerial vehicles (UAVs) have emerged in the last years and, albeit being sometimes notably smaller, yet they have to accomplish for the same certification process. This paper investigates into the possibility of using a reverberation chamber for performing two aircraft low-level coupling tests, namely, low-level direct drive and low-level swept fields, and compares the results with those obtained in an OATS, in both cases using a representative part of a UAV.**

***Index Terms*—Aircraft electromagnetic compatibility (EMC) certification, low-level direct drive (LLDD), low-level swept fields (LLSF), open area test sites (OATS), reverberation chambers.**

I. Introduction

THE impact of the electromagnetic environment upon the operational capability of aeronautic equipment is becoming bigger in modern air vehicles due to the increase of fly-by-wire systems in substitution of traditional mechanical options. Electromagnetic compatibility (EMC) certification, aimed to ensure air vehicles safety, imposes the fulfillment of a number of requirements prior to flying in the airspace, in terms of usual electromagnetic interference threats. Among them, and in relation to this study: the high-intensity radiated field (HIRF) effects. Every air vehicle must undergo a rigorous safety assessment in order to determine the criticality of every system and, thus, their appropriate HIRF certification levels. The certification applicant must demonstrate that the systems that perform or contribute to functions whose failure would result in a catastrophic, hazardous, or major failure conditions (Levels A, B, and C, respectively) comply to the HIRF regulation and are not adversely affected when the aircraft is exposed to an HIRF environment [1]–[3]. On this subject, unmanned aerial vehicles (UAVs) have attracted the attention of manufacturers in the last two decades and have experienced a notorious development since. Nowadays, UAV regulations are being developed by several countries taking into account different safety requirements, proportionate to the risks. For example, the European Aviation Safety Agency proposes a categorization of UAV operations in three categories, namely, open, specific, and certified, based on the risk of the operation [4]. Particularly, those operations classified as certified are intended to require the certification of the UAV, as well as a licensed remote pilot and an operator approved by the competent authority, in order to ensure an appropriate level of safety. The list of operations proposed to be classified as certified-category operations is still under development [5]. The certification requirements for the UAV in those cases will be similar to those for manned aircraft. International standards provide technical guidance to demonstrate that air vehicles comply with HIRF regulations from 10 kHz to 18 GHz [6], [7].

In this regard, there are two methods of evaluating the HIRF performance of a whole aircraft: traditional aircraft high-level tests or alternative aircraft low-level coupling tests. The former involves illuminating the aircraft with high-amplitude radio frequency (RF) fields to assess the effects on aircraft systems whereas the latter uses low-amplitude RF fields to determine the internal aircraft environment. The internal environment is then compared to the RF levels used during bench or high-level tests of Level A systems. The low-level coupling tests are mainly preferred now [6].

In any case, these kinds of tests need to be performed in dedicated test sites. Due to the size of aircraft, calibrated open area test sites (OATS) [8] have been routinely used for these purposes. But they are outdoor facilities and suffer from intrinsic disadvantages, probably the most important one being the necessity of dealing with the vagaries of weather. In addition, OATS are also exposed to electromagnetic environmental interference and, even, to overhead observation by aircraft or satellites, a significant problem with certain aircraft. As a result, alternatives to deal with EMC tests of such large items have been occasionally sought. Some authors have researched *in situ* approaches instead, either using a mobile laboratory and part of a hangar just as a shelter [9] or the hangar itself as the structure to form a reverberation chamber (RC) [10], [11]. This interesting on-site

Manuscript received May 22, 2017; revised July 24, 2017; accepted July 31, 2017. Date of publication January 18, 2018; date of current version August 13, 2018. This work was supported by the projects TEC2013-48414- C3-2-R and TEC2016-79214-C3-1-R (Spanish MINECO). *(Corresponding author: David Escot Bocanegra.)*

S. Fernández Romero and M. Añón Cancela are with the Electromagnetic Compatibility Area, National Institute for Aerospace Technology (INTA), Torrejón de Ardoz E-28850, Spain (e-mail: fdezrs@inta.es; agnonmc@inta.es).

P. López Rodríguez is with the AKKA Technologies, Madrid E-28027, Spain (e-mail: patricia.lopez@akka.eu.).

D. Escot Bocanegra and D. Poyatos Martínez are with the Radiofrequency Area, National Institute for Aerospace Technology (INTA), Torrejón de Ardoz E-28850, Spain (e-mail: escotbd@inta.es; poyatosmd@inta.es).

Color versions of one or more of the figures in this paper are available online at http://ieeexplore.ieee.org.

Digital Object Identifier 10.1109/TEMC.2017.2747771

concept continues to be explored in the EMC community [12]. On the other hand, comparisons of results obtained in different tests sites, no matter the application, are not that common and, despite notable efforts [13]–[15], they are specially scarce when dealing with aircraft [16] or with the particular case of OATS and RC [17].

In this context, the Spanish-funded project UAVEMI focuses on the numerical and experimental EM immunity assessment of UAVs for HIRF and lightning indirect effects [18]. This paper takes advantage of an opportunity arisen within that project and aims at comparing the results obtained when measuring part of a UAV in two test sites, an OATS and an RC. Two aircraft low-level coupling tests are studied in depth, namely, low-level direct drive (LLDD), and low-level swept fields (LLSF). In the case of LLDD, the coaxial return technique was employed instead of the classical ground return technique [19], [20] both in OATS and RC, but the RC was used only as a mere shelter, without moving the paddles. Thus, in this case, the aim was to confirm that the RC structure does not affect the results and that good agreement with OATS could be obtained. On the other hand, the LLSF tests were conducted in the RC with the paddles in stirrer mode and compared with the worst case result obtained for several illuminations in OATS. Although the object under test considered in this work is not as large as a full aircraft, the procedures applied are the same, and the conclusions can be extrapolated.

The paper is organized as follows: Section II sequentially includes the test object and the test measurement descriptions, Section III is devoted to the presentation of the results and the accompanying discussions, and finally, Section IV draws the conclusions.

II. Test Setup

A. Test Object Description

MILANO is a medium-altitude long-endurance remote-piloted aircraft system developed by the National Institute for Aerospace Technology (INTA), formed by a UAV and a ground-control station [21]. The MILANO UAV, made mostly in carbon-fiber composite, has a wingspan of 12.5 m, a length of 8.52 m, and a height of 1.43 m. The UAV structure consists of independent composite modules with metallic fittings in order to assemble and disassemble the aircraft for transport. Only the central fuselage was used for the work described in this paper, in dark blue in Fig. 1. The central fuselage has a length of 3.5 m and it has a top fairing that can be removed, exposing then three different bays or compartments. Four copper wires, with several lengths and routes simulating UAV bundles between different equipment, (in red in Fig. 2) were installed inside the central fuselage and were connected to different metallic parts. The big apertures of the central fuselage located at the bottom, left-hand side and right-hand side (see Fig. 3) were covered with metallic plates. It was decided not to install any UAV equipment during the tests. The reason is twofold. On one hand, the aim of this study was to focus on the comparison of the results obtained in two different test sites. In order to enable valid comparisons, easy access to the bays as well as easy manipulation of the mea-

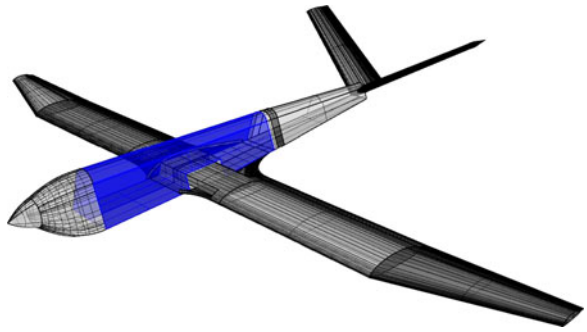

Fig. 1. MILANO UAV general view (CAD model). The central part of the fuselage employed in this work is highlighted in blue.

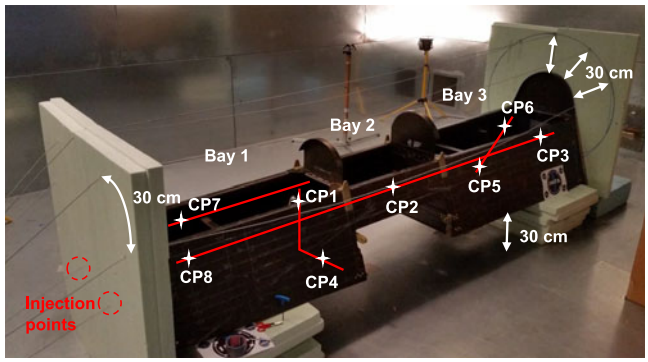

Fig. 2. LLDD RC test setup. The cables are depicted in red and the points where the induced current was measured are marked in white (CP1 to CP8). Note that the top fairing was removed for the photograph but was present during the test.

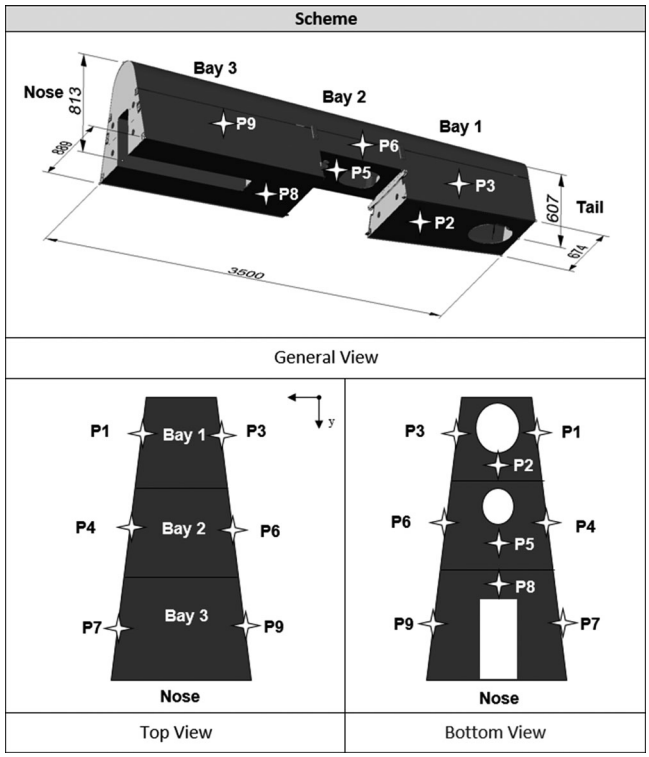

Fig. 3. Location of the points where the surface current was measured under the LLDD tests (both for RC and OATS). The openings at the bottom and in the nose were covered with metallic plates during the tests.

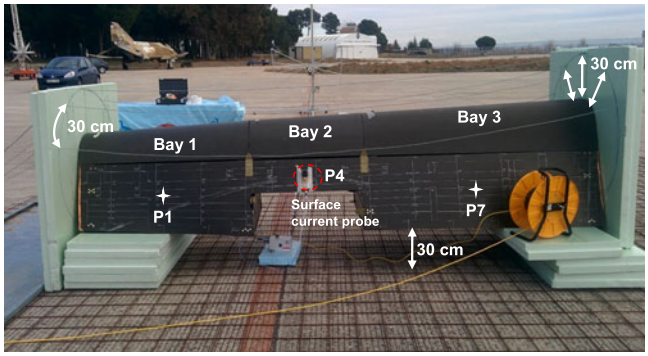

Fig. 4. LLDD OATS test setup. The setup is exactly the same as in Fig. 2 (location of the injection points, separation of the lines forming the coaxial lines, separation from the ground, location of the points where the induced current is measured.). The visible points where the surface current was measured (P1, P4, and P7) are also marked in the figure.

suring probes in several points should be granted. On the other hand, under the scope of the UAVEMI project, the experimental results would also be used for validation of numerical simulations based on finite difference time domain (FDTD) solvers that are trying to include the behaviour of composite materials in their calculations [22]. For this kind of validation exercise, a simplified test object model is preferred.

B. Test Measurement Description

The INTA EMC Area has different test facilities for EMC testing and in this work the OATS and one of the RC were used. The INTA OATS facility is a concrete built platform and its dimensions are $50\,\text{m} \times 50\,\text{m}$, whereas the INTA RC employed in these tests is a galvanized steel chamber sized $7.5\,\text{m} \times 5.6\,\text{m} \times 4.6\,\text{m}$ with two stirrers or paddles.

1) LLDD Tests: The objective of the LLDD tests is to obtain the transfer function relating the aircraft skin current to the current induced on the cable bundles. This technique is used in the EMC certification process from 10 kHz to the first resonance frequency of the aircraft. For LLDD tests, the guides [6], [7] recommend the design of a coaxial return wire network where the aircraft is considered the main conductor. In our case, the injected current and the surface currents in several positions of the fuselage were measured, as well as the current induced, from 10 kHz to 400 MHz, on the different copper wires installed inside the bays (the guides recommend to measure up to the first resonance but in this work, for the sake of comparison, this limit was increased). The coaxial return wire network was implemented through five copper wires and the conductive floor. The MILANO central fuselage was raised 30 cm from the RC or OATS floor using insulation panels made of polystyrene blocks or foam stands, as shown in Figs. 2 and 4. The RF power was injected to the MILANO central fuselage through two wires connected to two screws of the fuselage metallic fittings, marked in Fig. 2 with two red circles, in configuration nose to tail. The power was dissipated at an RF load located between the end of the fuselage and the coaxial return wire network.

According to [6] and [7], a complete set of measurements was carried out using this setup in the RC and it was repeated in the OATS. Prior to the LLDD test, the reflection coefficient S_{11} was measured in order to determine the mismatch between the amplifier output and the UAV/coaxial return wire network. After that, the current injected into the central fuselage to the 50Ω load was measured and recorded in order to normalize the surface currents and the currents induced on the internal cables. The signal to current injection fixture was driven from the port 1 of a vector network analyzer (VNA) with a constant power and amplified by means of a power amplifier always working in the linear region. The amplifier output power was recorded using a directional coupler and monitored during the test runs.

Multigap loop B-dot ground plane sensors were used for the surface current measurement at nine locations (called P1–P9, see Figs. 3 and 4). These sensors were connected to the port 2 of the VNA through a fiber optic link (FOL) and were placed in two orthogonal orientations. The first one, the so-called component y, goes along the fuselage, i.e., nose to tail, whereas the other one, the so-called component x, is perpendicular to it, i.e., encircling the fuselage. The vectorial magnitude of the total surface current (both components) was used for comparisons. Furthermore, the current induced on the internal wires was measured with calibrated current probes at eight different locations (called CP1–CP8, see Fig. 2), and, also, they were connected to the port 2 of the VNA through an FOL.

2) LLSF Tests: The objective of the LLSF tests is to measure the transfer function relating external RF fields to internal fields from 100 MHz to 18 GHz. Thus, the test consists of two phases according to [6] and [7] (for OATS) and [23] (for RC). First, the field from the transmitting (Tx) antenna is measured at the required location and the forward power fed to the antenna is recorded. This measurement is called the reference. After that, the aircraft is placed inside the test volume, the same forward power is fed to the radiating antenna and the fields inside different bays or cavities are measured. The outcome of the LLSF tests is the fuselage attenuation or shielding effectiveness (SE), defined as the ratio between the reference measurement and the measurements made inside the aircraft.

In our work, the internal RF E-field was measured at a fixed point inside each of the three bays from 200 to 18 000 MHz, and LLSF tests were carried out both in RC and OATS. The signal to the Tx antenna was driven from the port 1 of a VNA with constant power and it was amplified by means of four power amplifiers working from 200 MHz to 1 GHz, 1–4 GHz, 4–8 GHz, and 8–18 GHz, respectively. Two different Tx antennas were used, a log-periodic antenna from 200 MHz to 1 GHz and a broadband horn antenna from 1 to 18 GHz. The receiving (Rx) antenna should be small enough to be located inside the bays, so a small biconical antenna (top hat) was selected due to its reduced dimensions. This antenna is just 6 cm long by 3 cm of diameter and was designed for a frequency band from 1 to 18 GHz. However, in this trial, it was used for the whole frequency range (starting in 200 MHz) in spite of the expected worse performance in the lower band. The rationale is that the SE is a relative parameter and, then, receiving more than 6 dB over the noise floor is enough to obtain good measurement results, as shown in [24].

Fig. 5. LLSF RC test setup. The top-hat antenna used for measuring the reference appears in the foreground.

Fig. 6. LLSF OATS test setup. The figure shows a vertically polarized illumination from the starboard of the target.

The RC tests were conducted with the paddle in stirrer mode and a mean E-field was collected, according to [23]. The fields distribution inside an RC can notably change in the presence of the object under test, so it is recommended to measure the reference external field in the presence of the object. This is the case shown in Fig. 5. The receiving antenna was connected to port 2 of the VNA through an FOL. After measuring the reference, it was placed at the center of each compartment keeping the same positions for all the measurement repetitions.

On the other hand, the LLSF tests carried out in the OATS were conducted for four illumination angles, spaced 90 degrees (nose-on, tail-on, and both side-on) and for both horizontal and vertical polarizations. Additionally, the test was repeated placing the Tx antenna at two height positions with the fuselage placed 0.8 m over the platform floor. The worst case attenuation of these 16 situations was obtained. As the guides recommend [6], [7], it is important to ensure that all leakage points of the fuselage are illuminated with the field, that means the Tx antennas should be located far enough to ensure that all these leakage points are included in the antenna beamwidth. Given the size of the object and the beamwidth of the antennas used in this work, the log-periodic one was always located at 6 m from the UAV and the horn antenna at 7 m. Fig. 6 shows the LLSF measurement setup in the OATS. Regarding the reference, it was measured in the center of the platform without the UAV present for each transmitting antenna and polarization but only for one illumination angle and height. According to the guides, a single reference point suffices for all the illumination angles if the distance of the transmitting antennas complies with the aforementioned requirements.

III. Results and Discussion

A. LLDD

First of all, the coaxial return installation described in Section II-B1 was deployed in the RC. After the LLDD tests were concluded, the setup was disassembled and it was assembled again in the OATS. In both cases, the S_{11} was measured prior to the injection of the current and, later, this injected current was also recorded. The latter would then be used to normalize the measured surface currents and induced currents.

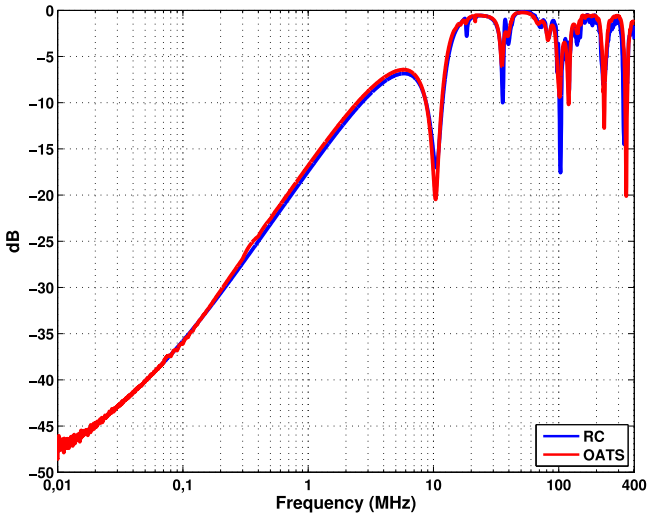

Fig. 7. Reflection coefficient comparison.

Fig. 7 shows the return losses whereas Figs. 8–11 present the surface current measured in points P1 and P4 (recall Figs. 3 and 4) and the current induced in points CP2 and CP7 (recall Fig. 2), respectively. The remaining measurement points yield similar comparisons. In general, the agreement is excellent in almost the whole frequency band except for small discrepancies at very low and very high frequencies. Remember that the guides recommend to measure up to the first resonance (here, as can be appreciated in Figs. 8–11, around 30 MHz) but the tests were conducted beyond this limit for the sake of comparison between sites. Even having increased the upper limit, the comparisons yield a notable agreement.

From these results, it can be concluded that the reproducibility of the test setup in both sites is very good from 10 kHz to hundreds of MHz. Here, the paddles were not moving and the RC is used as a mere shelter, but it has been confirmed that the

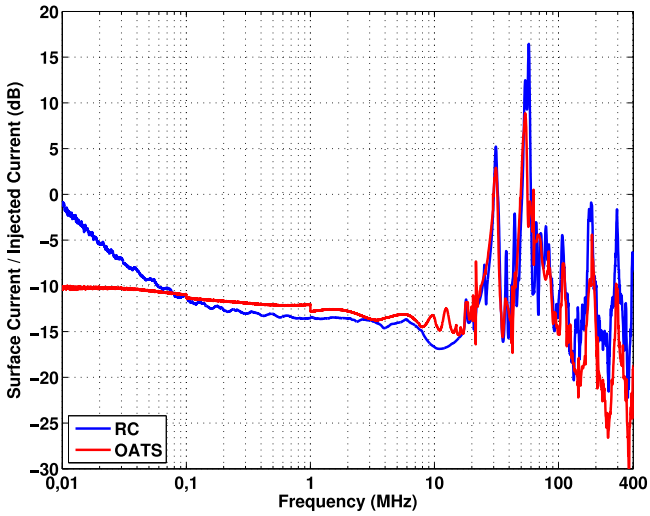

Fig. 8. P1 surface current comparison.

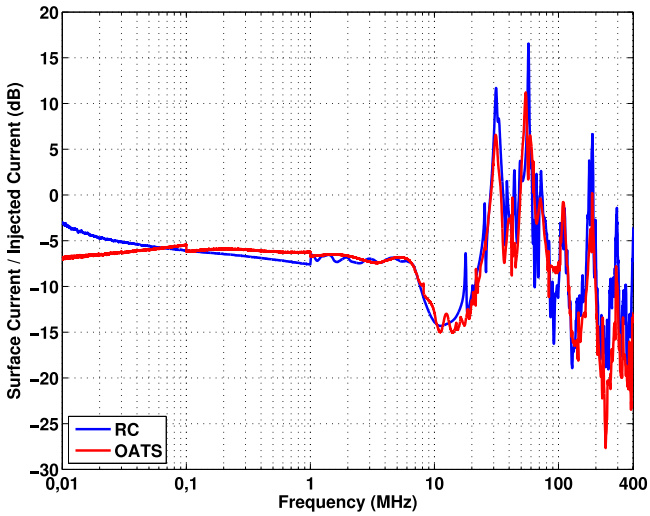

Fig. 9. P4 surface current comparison.

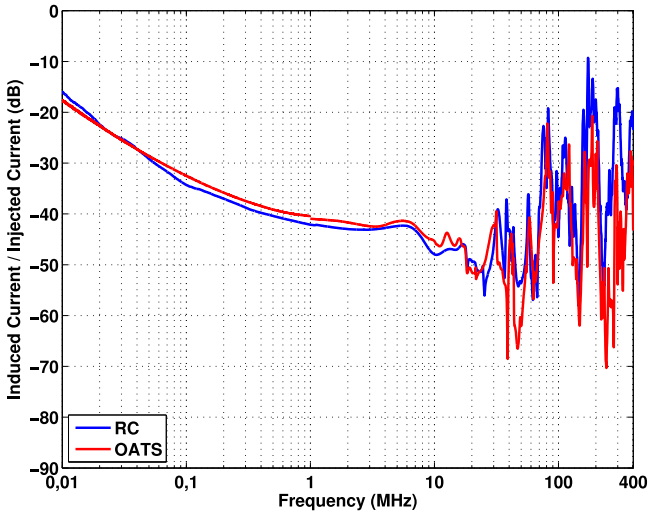

Fig. 10. CP2 induced current comparison.

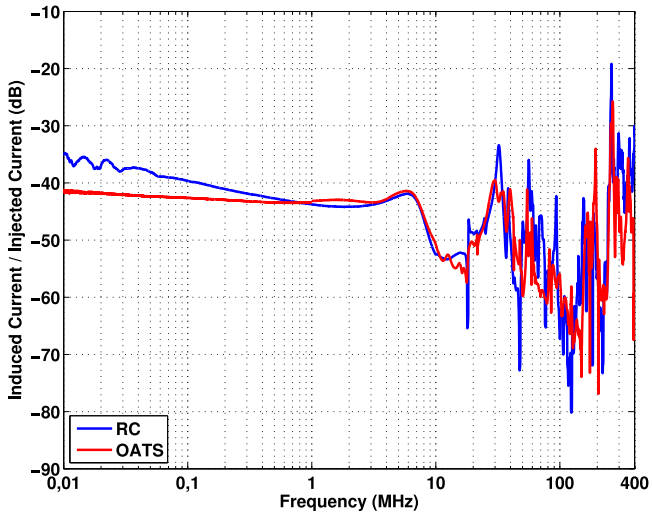

Fig. 11. CP7 induced current comparison.

coaxial line implies a good field concentration, independent of the environment, and the walls of the RC do not affect negatively to the results.

This characteristic is very important because of the inherent advantages of testing in a closed facility (i.e., an RC or a hangar) rather than in a open one (i.e., an OATS), in terms of weather and external RF interference protection, for instance.

B. LLSF

The LLSF tests were first conducted in the RC. The final SE results were calculated as the mean of 100 measurements stirring the chamber paddles. Also, an averaging filter of 5% of frequency was used, as recommended in [6] and [7]. The selection of the width of this filter depends on several factors including the number of modes and the quality factor of the chamber, among others [23], [25]. INTA has checked that a 5% is well suited for this test in this chamber [26]. Later, the LLSF tests were repeated in the INTA OATS. There, the final SE results were calculated as the worst case obtained from the 16 different measurements and the same averaging filter was used. Take into account that the worst case refers to the less attenuation, i.e., the lower SE. Note also that the number of different measurements in OATS is limited and, as a consequence, a reverberant environment is not granted. Under these circumstances, the mean of the different measurements tends to overestimate the SE and that is why the worst case option is commonly preferred. Figs. 12, 13, and 14 show the comparison of the SE results for the MILANO fuselage bays 1, 2, and 3, respectively.

Resonances can be observed in the three bays below 1 GHz (marked with a circle in the figures), where the number of modes present inside the cavities is very low due to their dimensions. On the other hand, the SE results are steadier above 1 GHz, where the electromagnetic environment is more reverberant. More in detail, if we analyze the RC data in the high frequency range, the compartments 1 and 3 show a slightly growing trend from 5 to 10 dB while the second bay shows averaged values around 5 dB. The measurement results in the OATS present similar trends

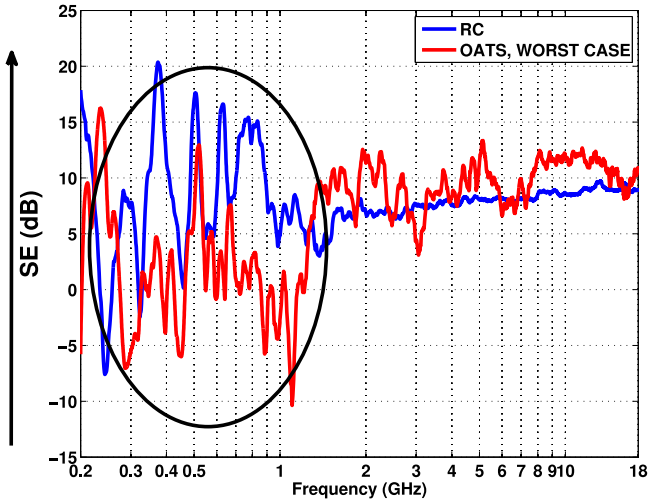

Fig. 12. Bay 1 SE comparison.

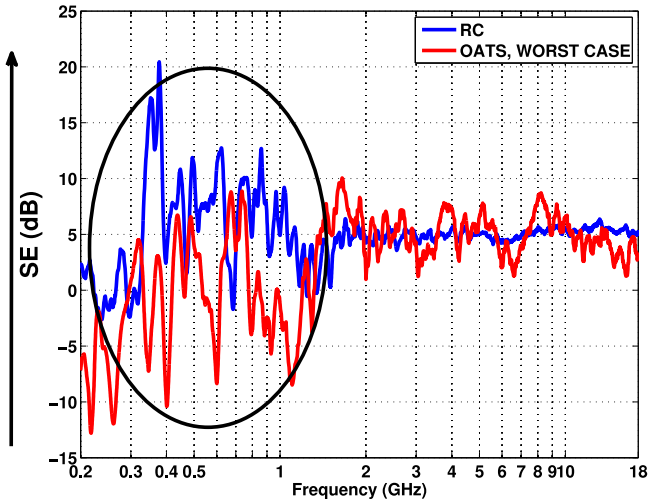

Fig. 13. Bay 2 SE comparison.

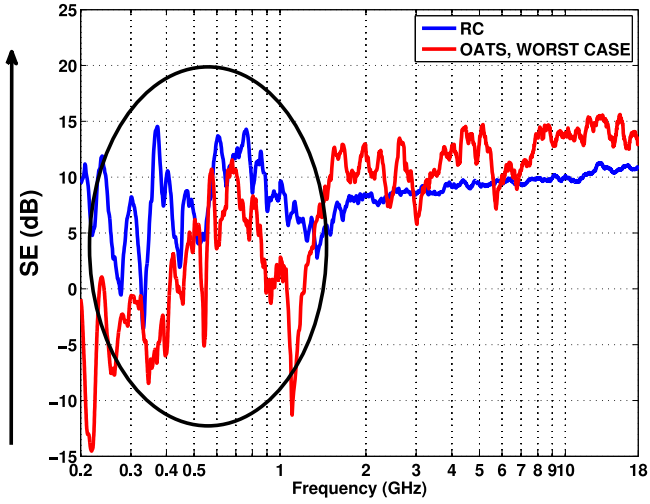

Fig. 14. Bay 3 SE comparison.

TABLE I
MINIMUM USABLE FREQUENCY FOR RC METHOD

	Volume (m^3)	Minimum frequency (MHz)
Fuselage	1.216	541.8
Bay 1	0.375	801.9
Bay 2	0.144	1103.3
Bay 3	0.697	652.2

and values. In the low frequency range, however, the comparison of the results is more difficult due to the different resonances measured with the two methods (RC and OATS).

In this regard, the two methods applied for the SE measurement have different advantages, drawbacks, and limitations. The most important limitation concerns the aircraft compartment sizes. The EM environment inside a cavity can be divided into three ranges. At very low frequency, when the cavity is small related to the signal wavelength, no transmission modes can exist inside. In the resonant frequency range, when the signal wavelength is similar to the cavity dimensions, there may be significant amplitude variations due to resonances or reflections. Finally, the high frequency range is considered when more than 60 modes are present and a reverberant EM environment is created inside the cavity. In order for a frequency stirring technique to be valid, the aircraft compartment shall be able to support at least 60 transmission modes for a given enclosure size and frequency. Then, the lowest usable frequency is given by the following formula [23]:

$$f_{\min} = c\left(\frac{90}{4\pi V}\right)^{1/3} \tag{1}$$

where V is the volume of the small enclosure and c the speed of light in free space. Table I shows the lowest usable frequency of the RC method using (1) for this case dimensions. However, this limit is not clearly defined for complex objects. For instance, the three compartments of the MILANO central fuselage are not completely independent because the RF energy can couple through different existing small apertures and, also, there is a copper wire connecting bay 1 and bay 3.

On the other hand, as it has been mentioned before, for the SE measurements in OATS, the distance from the transmitting antennas to the aircraft should be far enough to ensure that all leakage points are included in the antenna beamwidth. When the aircraft is huge, it is hard to meet with this illumination area requirement but easier to find a receiving antenna for the whole frequency range because the antenna size poses no problem. In contrast, when the aircraft is small, as is the case of this paper, it is easier to meet the illumination area requirement but harder to find a receiving antenna small enough for the aircraft cavities (the use of low-gain antennas is a possible solution and the one chosen in this work). An additional drawback of this method is that the number of illumination angles and polarizations are limited and the data can only be postprocessed in order to obtain the SE of the worst case. For these reasons, the SE calculated in OATS fluctuates more and, in the resonant frequency range,

even unrealistic results (SE < 0) can be easily obtained with this method, as shown in Figs. 12, 13, and 14. Consequently, the RC approach for determining the SE of a UAV is considered by the authors more reliable.

IV. Conclusion

This paper has presented a comparison between the results obtained in two different test sites, namely an RC and an OATS, for LLDD and LLSF measurements on a representative part of a UAV.

For the LLDD tests, a coaxial return was utilized as opposed to the classical ground return. The main advantages of an LLDD test using the coaxial return technique are a better surface current homogeneity, a better reflection coefficient and good field concentration, independent of the test site, which implies good reproducibility. In the case of the RC, the paddles were not moving and, thus, the RC was indeed employed as a shelter. The tests have shown that under these circumstances the results obtained both inside (RC) and outside (OATS) a chamber are quite comparable. This is indeed a good point because, overall, it is better to carry out a long test campaign in a closed facility (e.g., a hangar) due to its inherent independence from bad weather conditions or the protection from an RF interference environment or even, in some cases, indiscreet eyes. And it is not that difficult to find an RC or similar closed facility where these tests can be carried out due to the reduced dimensions of a UAV.

As for the LLSF tests, the aim of the paper was to deepen the knowledge of the guides and standards and to check the advantages and drawbacks related to two different methods (RC and OATS) of measuring the same parameter (SE of a UAV). Regulations permit to perform the test either following RC or OATS procedures but in both cases a statistical approach is recommended. In general, no matter the method, the figures have shown a noticeable different behavior at low and high frequency. When the frequency rises (above around 1 GHz), the cavities of the object support a bigger number of transmission modes and the response is smoother. In contrast, at lower frequencies, the response is more erratic.

However, there are discrepancies between the results obtained with OATS and RC. Below the lowest usable frequency, the RC method is not really valid according to the standards whereas the guides for OATS are not that clear regarding low frequencies. Albeit this, it is worth noting that the results obtained in RC in this band are more reasonable than those obtained in OATS (values of SE < 0 appear more frequently in OATS). In any case, below 1 GHz, the authors reckon that is it difficult to extract conclusions given the limitations of both procedures. On the other hand, at high frequency, although there are also differences between both methods, the results obtained in RC are smoother and are the consequence of a true reverberant environment that is not produced in OATS, given the limited number of scenarios. The RC method easily enables a sufficient number of different incident angles and polarizations and, thus, a better statistical environment with less effort. In fact, the main advantages of the RC method for LLSF tests are significant time savings and a better test rigor subjecting the object to a multipath environment, yielding statistical results, rather than deterministic results that need to be mixed afterwards.

Finally, regarding the extrapolation to bigger test objects, e.g., an aircraft, the following initial remarks can be done, depending on the test. In LLDD, our results indicate that a chamber big enough to accommodate the object under test and the associated coaxial return setup would apparently suffice.

Concerning the LLSF tests, first, the size of the RC should be big enough to accommodate the object inside the working volume of the chamber. Then, it has to be taken into account that the lowest usable frequency would depend on the size of the bays or compartments to be tested. But no other limitations are currently foreseen.

References

[1] *"The Certification of Aircraft Electrical and Electronic Systems for Operation in the High-intensity Radiated Fields (HIRF) Environment,"* FAA Advisory Circular 20–158A, May 2014.

[2] *"Environmental Conditions and Test Procedures for Airborne Equipment,"* RTCA DO 160G, Jun. 2011.

[3] *"Requirements for the Control of Electromagnetic Interference Characteristics of Subsystems and Equipment,"* MIL-STD-461G, December 2015.

[4] EASA civil drones (unmanned aircraft). [Online]. Available: https://www.easa.europa.eu/easa-and-you/civil-drones-rpas. Accessed on: Jul. 2017.

[5] EASA Notice of Proposed Amendment 2017-05 (A). [Online]. Available: https://www.easa.europa.eu/system/files/dfu/NPA%202017-05%20%28A%29_0.pdf. Accessed on: Jul. 2017

[6] *"Guide to Certification of Aircraft in a High Intensity Radiated Field (HIRF) Environment,"* A ed., SAE ARP 5583, Jun. 2010.

[7] *"Guide to Certification of Aircraft in a High Intensity Radiated Field (HIRF) Environment,"* EUROCAE ED-107A, Jul. 2010.

[8] S. Eser and L. Sevgi, "Open-area test site (OATS) calibration," *IEEE Antennas Propag. Mag.*, vol. 52, no. 3, pp. 204–212, Jun. 2010.

[9] B. M. Kent *et al.*, "Electromagnetic interference attenuation test of the space shuttle discovery using the air force research laboratory mobile diagnostic laboratory," *IEEE Antennas Propag. Mag.*, vol. 47, no. 6, pp. 128–134, Dec. 2005.

[10] M. O. Hatfield, W. P. Pluim, and W. Price, "Investigation into in-situ shielding effectiveness testing of transport aircraft," in *Proc. IEEE Int. Symp. Electromagn. Compat.*, 2003, vol. 1, pp. 414–418.

[11] G. Andrieu, F. Tristant, and A. Reineix, "Investigations about the use of aeronautical metallic halls containing apertures as mode-stirred reverberation chambers," *IEEE Trans. Electromagn. Compat.*, vol. 55, no. 1, pp. 13–20, Feb. 2013.

[12] R. Vogt-Ardatjew, U. Lundgren, S. F. Romero, and F. Leferink, "On-site radiated emissions measurements in semireverberant environments," *IEEE Trans. Electromagn. Compat.*, vol. 59, no. 3, pp. 770–778, Jun. 2017.

[13] K. Hall, D. Pommerenke, and L. Kolb, "Comparison of site-to-site measurement reproducibility using UK National Physical Laboratory and Austrian Research Center test sites as a reference," in *Proc. IEEE Int. Symp. Electromagn. Compat.,* 2000, vol. 2, pp. 939–943.

[14] K. Osabe, R. Watanabe, A. Maeda, and M. Yamaguchi, "Inter-laboratory comparison result as the proficiency testing program of EMI test sites in japan," in *Proc. IEEE Int. Symp. Electromagn. Compat.*, 2007, pp. 1–6.

[15] E. Amador, C. Miry, and N. Bouyge, "Compatible susceptibility measurements in fully anechoic room and reverberation chamber," in *Proc. Int. Symp. Electromag. Compat.*, 2014, pp. 860–865.

[16] E. J. Borgstrom, "A comparison of methods and results using the semi-anechoic and reverberation chamber radiated RF susceptibility test procedures in RTCA/DO-160d, change one," in *Proc. IEEE Int. Symp. Electromagn. Compat.*, 2002, vol. 1, pp. 184–188.

[17] M. Hoijer and M. Backstrom, "How we confused the comparison between high level radiated susceptibility measurements in the reverberation chamber and at the open area test site," in *Proc. IEEE Int. Symp. Electromagn. Compat.*, 2003, vol. 2, pp. 1043–1046.

[18] S. G. Garcia *et al.*, "UAVEMI project: Numerical and experimental EM immunity assessment of UAV for HIRF and lightning indirect effects," in *Proc. 2016 ESA Workshop Aerosp. EMC*, May 2016, pp. 1–5.

[19] *Aircraft Lightning Test Method*, EUROCAE ED-105A, Jul. 2013.

[20] M. Rothenhausler, A. Ruhfass, and T. Leibl, "Broadband DCI as a multi usable EMC-test method," in *Proc. 2008 IEEE Int. Symp. Electromagn. Compat.*, Aug. 2008, pp. 1–5.
[21] MILANO system. [Online]. Available: http://www.inta.es/opencms/export/sites/default/INTA/en/quienes-somos/historia/los-rpa/. Accessed on: Jul. 2017.
[22] M. R. Cabello *et al.*, "SIVA UAV: A case study for the EMC analysis of composite air vehicles," *IEEE Trans. Electromagn. Compat.*, vol. 59, no. 4, pp. 1103–1113, Aug. 2017.
[23] *IEEE Standard Method for Measuring the Shielding Effectiveness of Enclosures and Boxes Having All Dimensions Between 0.1 m and 2 m*, IEEE Std 299.1-2013, Oct. 2013.
[24] S. Fernandez, G. Gutierrez, and I. Gonzalez Diego, "A shielding effectiveness prediction method for coupled reverberant cavities validated on a real object," *J. Electromagn. Waves Appl.*, vol. 29, no. 14, pp. 1829–1840, 2015.
[25] C. L. Holloway *et al.*, "Use of reverberation chambers to determine the shielding effectiveness of physically small, electrically large enclosures and cavities," *IEEE Trans. Electromagn. Compat.*, vol. 50, no. 4, pp. 770–782, Nov. 2008.
[26] S. F. Romero, G. G. Gutierrez, and I. Gonzalez, "Prediction of the maximum electric field level inside a metallic cavity using a quality factor estimation," *J. Electromagn. Waves Appl.*, vol. 28, no. 12, pp. 1468–1477, 2014.

Sergio Fernández Romero was born in Valencia, Spain, in 1978. He received the M.S. degree in telecommunication engineering from the University of Valencia, Valencia, Spain, in January 2002, and the Ph.D. degree in telecommunication engineering from the University of Alcala, Madrid, Madrid, Spain, in 2016.

Since 2003, he has been with the electromagnetic compatibility (EMC) on Aircraft Test Group, National Institute for Aerospace Technology, Torrejon de Ardoz, Madrid, Spain. His current research interest include reverberation chambers, EMC and shielding effectiveness measurements, and some related topics such as time domain measurements and reverberant microwave propagation models.

Dr. Romero is a member of the International Electrotechnical Commission joint task force on reverberation chambers.

Patricia López Rodríguez was born in Murcia, Spain in 1986. She received the M. Sc. degree in telecommunications engineering from the Technical University of Cartagena, Murcia, Spain, and the Ph.D. degree from the University of Alcalá, Madrid, Spain, in 2010 and 2016, respectively. She joined INTA in 2011, first as a Ph.D. student, and then as a Researcher. In 2016, she joined AKKA Technologies, Madrid, Spain, where she works as a subcontractor for Airbus Defense and Space in the Department of EME & Antennas Systems Engineering. Her main activities and research interests include electromagnetic compatibility, radar cross section, radar imaging, and pattern recognition.

David Escot Bocanegra was born in Madrid, Spain, and received the M.Sc. and Ph.D. degrees in telecommunication engineering from the University of Alcalá, Madrid, Spain, in 2002 and 2012, respectively.

From 2002 to 2003, he was a Junior Researcher with Telecom Bretagne, Brest, France.

In 2004, he joined INTA, Spain, first as a Researcher and is currently a Scientist with the Radiofrequency Area. He has authored or coauthored numerous refereed journal articles and has been principal investigator in serveral national and international research projects. His research interests are related to radar cross section, computational electromagnetics, materials characterization, and EMC simulations.

David Poyatos Martínez was born in Madrid, Spain. He received the M.Sc. degree from the Universidad Politécnica de Madrid, Madrid, Spain, and the Ph.D. degree from The University of Alcalá, Madrid, Spain, both in telecommunication engineering in 1998 and 2017, respectively.

He joined INTA, Spain, in 1997 as a Junior Research Assistant with the EMC Area. In 2000, he became R&D+i Engineer with the Detectability & Electronic Warfare Lab. He is currently the Head of the Radiofrequency Area, INTA. His current research activities and interests include the theoretical and practical study of radar reflectivity, the electromagnetic characterization of materials, and the application of numerical methods to electromagnetics, including the use of bio-inspired algorithms. He has authored more than 35 publications in books, journals, and conferences.

Manuel Añón Cancela was born in Carballo-A Coruña. He received the M.Sc. degree in physics from the Universidade de Santiago de Compostela La Coruña, Spain, in 1989.

He joined INTA in 1991 as E3 Test Engineer in the Electromagnetic Compatibility Area being involved in several national and international projects for the aerospace and defence sectors. He is currently the Head of the Electromagnetic Compatibility Area, INTA.

He is member of national and international standardization groups for military and civilian E3 specs.